

PAPER

Embed-Search-Align: DNA Sequence Alignment using Transformer models

Pavan Holur,^{1,†} K. C. Enevoldsen,^{2,3,†} Shreyas Rajesh,¹ Lajoyce Mboning,⁴
Thalia Georgiou,⁵ Louis-S. Bouchard,⁴ Matteo Pellegrini⁶
and Vwani Roychowdhury^{1,*}, †

¹Department of Electrical and Computer Engineering, UCLA, ²Center for Humanities Computing, Aarhus University, ³Center for Quantitative Genetics and Genomics, Aarhus University, ⁴Department of Chemistry and Biochemistry, UCLA, ⁵Department of Biochemistry, Biophysics, and Structural Biology (MBIDP), UCLA and ⁶Molecular, Cell, and Developmental Biology, UCLA
*Corresponding author. vwani@g.ucla.edu

FOR PUBLISHER ONLY Received on Date Month Year; revised on Date Month Year; accepted on Date Month Year

Abstract

DNA sequence alignment involves assigning short DNA reads to the most probable locations on an extensive reference genome. This process is crucial for various genomic analyses, including variant calling, transcriptomics, and epigenomics. Conventional methods, refined over decades, tackle this challenge in two steps: genome indexing followed by efficient search to locate likely positions for given reads. Building on the success of Large Language Models (LLM) in encoding text into embeddings, where the distance metric captures semantic similarity, recent efforts have explored whether the same Transformer architecture can produce numerical representations for DNA sequences. Such models have shown early promise in tasks involving classification of short DNA sequences, such as the detection of coding- vs non-coding regions, as well as the identification of enhancer and promoter sequences. Performance at sequence classification tasks does not, however, translate to *sequence alignment*, where it is necessary to conduct a genome-wide search to align every read successfully. We address this open problem by framing it as an “Embed-Search-Align” task. In this framework, a novel encoder model *DNA-ESA* generates representations of reads and fragments of the reference, which are projected into a shared vector space where the read-fragment distance is used as a surrogate for alignment. In particular, *DNA-ESA* introduces: (1) Contrastive loss for self-supervised training of DNA sequence representations, facilitating rich sequence-level embeddings, and (2) a DNA vector store to enable search across fragments on a global scale. *DNA-ESA* is 99% accurate when aligning 250-length reads onto a human reference genome of 3 gigabases (single-haploid), rivaling conventional algorithmic sequence alignment methods such as *Boutie* and *BWA-Mem*. *DNA-ESA* far exceeds the performance of 6 recent DNA-Transformer model baselines such as *Nucleotide Transformer*, *Hyena-DNA*, and shows task transfer across chromosomes and species.

Key words: Transformers, DNA Sequence Alignment, Large Language Models, Vector Stores

Introduction

Sequence alignment is a central problem in the analysis of sequence data. Many DNA sequencers generate short reads that are only a couple of hundred bases long. In order to interpret this data, a typical first step is to align the reads to a genome. Genomes come in many sizes, but many of the most commonly studied genomes, such as that of humans, are three gigabases long. Moreover, most experiments will generate millions of reads. Therefore, the resulting task of aligning reads to genomes is computationally expensive, and many decades of work have led to optimized approaches that can perform these

tasks with great efficiency. However, many limitations remain with existing genome alignment methods. One limitation is that a reference genome usually is an approximation of the sequence from a single individual, and does not capture the variability of genomes across populations. Another, is that sequence alignment algorithms may not correctly model sequencing errors, and thus may introduce mistakes when trying to score the best match for a sequence against a genome. We asked whether some of these limitations could potentially be overcome if we utilize a new paradigm to align reads to genomes by exploiting the Transformer architectures [45] adopted for recent language modeling efforts. The applications of the Transformer model – and, more generally “Large Language Models” (LLM) – in Bioinformatics applications are still in their infancy, yet hold substantial promise: Transformer models have demonstrated

†Equal Contribution

an unprecedented ability to construct powerful numerical representations of sequential data [14, 1, 4].

We establish a foundation model [3] tailored for DNA sequences, where the vocabulary consists of only a few symbols ($\{A, T, G, C\}$ in this case). Numerous DNA Transformer models [22, 51, 15, 11] have emerged recently, mainly designed for classification tasks in downstream applications. However, these models do not explicitly consider a fundamental distinction between Limited Vocabulary Languages (LVL) (such as genomes) and natural languages with large vocabulary. In LVLs, there is a one-to-one correspondence between the precise symbol ordering and the underlying “meaning”. If a protein is encoded by one amino acid sequence, a slightly different sequence (with a few edits) would encode for a different protein with a distinct functionality in the cells. Existing foundation Transformer models, trained on classification tasks, generate sequence embeddings such that their pairwise distances correspond to class separation. As a result, pairs of sequences with very large edit distances between them are mapped to numerical representations that are close by. There are, however, tasks such as Sequence Alignment where the objective is quite different: *the pairwise representation distance has to closely match the sequence edit distance*. Indeed as portrayed in Figure 1, current DNA Transformer models without any further refinement are unable to perform *Sequence Alignment* tasks: the representation space is simply not designed for such an objective. This demonstrates the need for a new model which is able to transfer a precise and computationally expensive distance metric, such as the edit distance, over LVLs to a continuous representation space.

The simplest sequence alignment task applies to single-end¹ reads, where a sequencer generates a read of length Q

$$r := (\bar{b}_1, \bar{b}_2, \dots, \bar{b}_Q), \quad (1)$$

where $\bar{b}_i \in \{A, T, G, C\}$. In practice, these reads come from individual genomes that do not necessarily match the reference and may contain mutations due to base insertions, deletions, and substitutions. Thus, it is assumed that this read is a noisy substring taken from a reference genome sequence $\mathcal{R} := (b_1, b_2, \dots, b_N)$, $b_i \in \{A, T, G, C\}$ and $N \gg Q$; for example, for the single-haploid human genome [37], $N \approx 3$ gigabases (gb), and $Q \approx 250$ though reads of much longer lengths are becoming increasingly affordable and accurate [50]. The alignment task is to find a substring in \mathcal{R}

$$\bar{r} := (b_q, b_{q+1}, \dots, b_{q+Q}), \quad 1 \leq q \leq N - Q, \quad (2)$$

such that the edit distance $d(r, \bar{r})$ – for example the Smith-Waterman (SW) distance – is minimized. The primary objective is to identify the most probable location, q , of this read within the reference genome.

Computational simulators have been developed to generate synthetic reads that have properties of real reads. These simulators mimic the read quality and characteristics produced by actual sequencing machines, thus providing a scalable means for validating new alignment approaches [19].

Conventional sequence alignment methods, such as those used in BWA-MEM, have evolved significantly from the basic SW approach, which computes the similarity between a read r and reference \mathcal{R} ; using the SW distance on its

own, however, is computationally intensive for large genomes. Some key advances include: (a) *Sharding* the reference into smaller fragments for individual searching; (b) *Progressive search* using phylogenetic trees and distance heuristics for logarithmic complexity scaling; (c) *Compression techniques* like the Burrows-Wheeler transform [28], reducing the effective search length; and (d) *Multi-core/thread implementations and database instantiations* for faster computations and improved data recall [27, 44, 25].

In this work, we explore an alternative paradigm for aligning a read to a genome, drawing parallels with advancements in Natural Language Processing (NLP). Traditional NLP relied on rule-based techniques to diagram sentences into grammatical components, using dependency parse trees to discern semantic relationships. However, the introduction of models like the Transformers [45] revolutionized this approach. Unlike rule-based frameworks, Transformers implicitly identify syntactic and semantic structures [43], as evidenced by their performance at various NLP tasks like Sentiment Analysis, Entity Recognition, and Question-Answering [12, 40, 39]. The flexibility of this architecture has facilitated its application beyond language processing, including in vision [13], auditory [46], and neurological domains [47]. In bioinformatics, researchers are now harnessing Transformers to bypass genome-specific hard-coded rules, a development we contribute to with our novel method for Sequence Alignment.

Transformer models: Written Language to DNA Sequence Alignment

DNA sequences share remarkable similarities with written language, offering a compelling avenue for the application of Transformer models. Like written language, these are sequences generated by a small alphabet of nucleotides $\{A, T, G, C\}$. Classical DNA modeling efforts have already accommodated mature encoding and hashing techniques initially developed for written language – such as Suffix trees/arrays and Huffman coding [20, 32] – to successfully parse and compress DNA sequences. Furthermore, just as written language contains repeated subsequences (words, phrases) to represent real-world objects, DNA sequences similarly possess repeating “words” and groupings of such words into a “sentence” representing, for example, subsets of genes.

Within the last few years, several Transformer-based models have been developed for DNA sequence analysis. Notably, DNABERT-2 [22, 48], Nucleotide Transformer [11], GenSLM [51], HyenaDNA [36] and GENA-LM [15] have been designed to discern relationships between short genetic fragments and their functions. Specifically, Nucleotide Transformer representations have shown utility in classifying key genomic features such as enhancer regions and promoter sequences. Similarly, GENA-LM has proven effective in identifying enhancers and Poly-adenylation sites in *Drosophila*. In parallel, DNABERT-2 representations have also been found to cluster in the representation space according to certain types of genetic function. Given these advances, a natural question arises: *Can these Transformer architectures be readily applied to the task of Sequence Alignment?* We delineate the associated challenges as follows:

[L1] Two-Stage Training: DNA-based Transformer models typically undergo pretraining via a *Next Token/Masked Token Prediction* framework, a method originally developed for natural language tasks. To form sequence-level representations, these models often employ pooling

¹ A DNA fragment is ligated to an adapter and then sequenced from one end only.

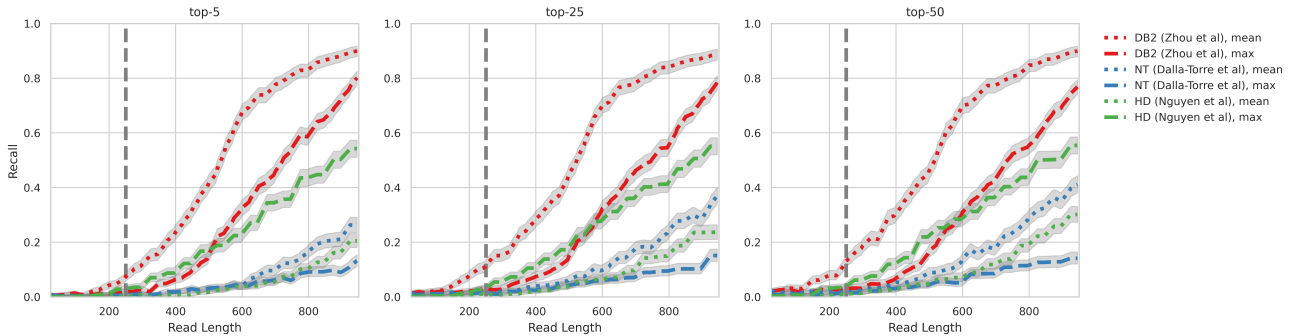


Fig. 1. Alignment Recall of Transformer-DNA Baselines by Read Length: Existing Transformer-DNA models were adapted for sequence alignment using mean-/max-pooling. Their performance, measured by recall (top- K) over $40K$ reads of varying lengths across the human genome (3gb - single-haploid), is shown. Trendlines represent each baseline, with error bars (Clopper-Pearson Interval [8] @ 95%) in grey. The vertical line at $x = 250$ marks a typical read length. Overall, these baselines show suboptimal performance. For more details, see Sec. 3.



(a) Three 20,000-long nucleotide sequences were selected, one each from Chr. 1, 2, and 3. Each sequence is broken up into 100 *consecutive* reference fragments, each of length 1000. Consecutive fragments have an overlap of 800 bases (stride 200). Additionally, reads of length $Q \sim \mathcal{U}[100, 250]$ are sampled from within each fragment. The colors correspond to the respective chromosomes and the position of a particular fragment along the 20K-nucleotide sequence is coded by its color intensity.

(b) Five gene regions (listed above in the inset) of different sizes are selected from the reference genome. Each gene is broken up into consecutive fragments of length 1000 with a stride of 200 (similar to subfigure (a)). Additionally, reads of length $Q \sim \mathcal{U}[100, 250]$ are sampled from within each fragment. The colors correspond to genes and the position of a particular fragment along a specific gene is coded by its color intensity.

Fig. 2. Illustrating DNA-ESA’s Preservation of Sequence Locality in Embedding Space: In DNA-ESA, the reference genome \mathcal{R} is divided into fragments \mathcal{F}_i , each represented by an embedding $h(\mathcal{F}_i)$. For effective sequence alignment, specific structures are expected in the embedding space: (1) Overlapping fragments \mathcal{F}_i and \mathcal{F}_j should have proximate embeddings; (2) Consecutive fragments forming a long sequence should correspond to a distinct manifold in the embedding space. Subfigures (a) and (b) display this emergent geometry, as visualized using DNA-ESA. In both subfigures, the fragment and read representations are jointly visualized in a 2D low-dimensional space constructed by applying UMAP [33] to the original embeddings. Vertical marker lines (|) refer to fragments, “—” markers correspond to reads. We observe that the consecutive fragments belonging to the same nucleotide (subfigure (a)) or gene (subfigure (b)) sequence constitute an order-preserving 1D manifold. Additionally, *almost all of the reads* are close to their corresponding fragments, making this space viable for the task of Sequence Alignment: by searching for fragments in the neighborhood of an external read represented in the embedding space, one is likely to retrieve a fragment most responsible for the read.

techniques that aggregate token-level features into a single feature vector. This approach, however, is sometimes critiqued for yielding suboptimal aggregate features [40].

[L2] Computation Cost: The computational requirements for Transformer models grow quadratically with the length of the input sequence. This is particularly challenging for sequence alignment tasks that necessitate scanning entire genomic reference sequences.

Figure 1 shows the sequence alignment performance (recall) of several Transformer-DNA models. The testing protocols are elaborated in Sec. 3. Notably, these models exhibit subpar recall performance when aligning typical read lengths of 250.

Our Contributions

In this paper, we argue that both limitations **L1**, **L2** of Transformer-DNA models can be mitigated by formulating sequence alignment as a vector search-and-retrieval task. Our approach is twofold: (A) We introduce a sequence encoder *DNA-ESA*, trained through self-supervision, to map DNA reads to relevant fragments in a reference sequence within a shared embedding space. (B) We leverage a specialized data structure, termed a *DNA vector store*, as a memory bank². This provides efficient access to the entire reference sequence for each read alignment. These strategies have been explored in NLP: (A) Sequence-to-embedding training using contrastive loss has shown improved performance – over explicit

² Codebase available here: <https://anonymous.4open.science/r/dna2vec-7E4E/>

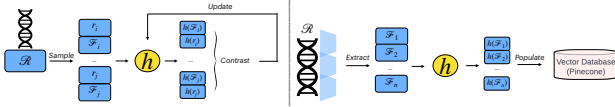


Fig. 3. System Overview [A] - Training Encoder and Populating Vector Store: Reference genome fragments \mathcal{F}_i and within them, randomly sampled pure reads r_i (positive pairs) are numerically represented via shared encoder h . Encoder training follows a contrastive approach as per (6). After training, the genome is segmented into overlapping fragments, encoded, and uploaded into the vector store.

pooling methods – at abstractive semantic tasks such as evidence retrieval [26] and semantic text similarity [16, 5]. (B) Specialized data structures, such as “vector stores” or “vector databases” like FAISS [23] and *Pinecone*, use advanced indexing and retrieval algorithms for scalable numerical representation search.

Task Definition

We formulate the problem of Sequence Alignment as minimizing a sequence alignment function, SA , applied to a read r and a reference sequence \mathcal{R} as

$$v^* = \min_q \text{SA}(r, \mathcal{R}) \quad (3)$$

where $q \in \{1, 2, 3, \dots\}$ is a candidate reference starting position and v^* is the optimal alignment score. Lower scores indicate better alignments. This optimization exhibits the following property:

Sharding for sequence alignment: For a read segment r of length Q and reference \mathcal{R} of length N , the complexity of $\text{SA}(r, \mathcal{R})$ scales as $\mathcal{O}(NQ)$, which is expensive.

Ideally, we would like to use \mathcal{R} to get a set of fragments $\{\mathcal{F}_1, \mathcal{F}_2, \dots, \mathcal{F}_K\}$ that are a subset of the original reference. Then:

$$v^* \approx \min_{\mathcal{F}_i \in \{\mathcal{F}_1, \mathcal{F}_2, \dots, \mathcal{F}_K\}} \text{SA}(r, \mathcal{F}_i). \quad (4)$$

Here, each \mathcal{F}_j is a fragment of \mathcal{R} (i.e., $\mathcal{F}_j \subset \mathcal{R}$), and K is the number of these sub-tasks. This approximation is effective under the conditions:

- (1) Fragment \mathcal{F}_j lengths are on the order of the read length (Q), and not the length of the longer reference \mathcal{R} ;
- (2) There are enough fragments \mathcal{F}_i to cover \mathcal{R} , i.e. $\cup \mathcal{F}_j = \mathcal{R}$;
- (3) K is significantly smaller than $\frac{N}{Q}$. If $\frac{N}{Q}$ then this amounts to scanning the whole reference.

Conditions (1) and (2) imply that fragments should be short and numerous enough to cover the reference genome. Condition (3) restricts the number of retrieved reference fragments per read — that we deem to be most likely to contain r — to a small value K . Analogous methods have shown efficacy in text-based Search-and-Retrieval tasks [38, 10] on Open-Domain Question-Answering, Ranking among other tasks. Subsequent sections describe a parallel framework for retrieving reference fragments given a read. The pipeline is shown in Figs. 3 and 4.

Designing effective sequence representations

An optimal sequence encoder model h is such that the corresponding embeddings of any read r and reference fragment $\mathcal{F} - h(r), h(\mathcal{F})$ respectively – obey the following constraints

over a pre-determined distance metric d :

$$d\{h(r_j), h(\mathcal{F}_i)\} \geq d\{h(r_j), h(\mathcal{F}_j)\}, \quad i \neq j \quad (5)$$

Here i and j serve to distinguish whether a read is aligned to a particular reference fragment, a *positive* sample $\{r_j, \mathcal{F}_j\}$, or there is a mismatch (*negative sample*): $\{r_j, \mathcal{F}_i\}$. Observe that these inequalities constitute the only requirements for the encoder. As long as the *neighborhood* of r_j in the representation space *contains* the representation for \mathcal{F}_j , it will be recovered in the nearest neighbors (top- K set) and alignment will succeed. Equality is observed when r_j is a repeat sequence matched equally well to more than one fragment. This motivates using self-supervision [18, 5, 16] where we are only concerned about the relative distances between positive and negative (read, reference fragment) pairs.

Self-supervision and contrastive loss

A popular choice for sequence learning using self-supervision involves a contrastive loss setup described by [5] and [16]: i.e. for a read r aligned to reference fragment \mathcal{F}_j , the loss l_r simultaneously minimizes the distance of $h(r)$ to $h(\mathcal{F}_j)$ and maximizes the distance to a batch of random fragments of size $B - 1$:

$$l_r = -\log \frac{e^{-d(h(r), h(\mathcal{F}_j))/\tau}}{e^{-d(h(r), h(\mathcal{F}_j))/\tau} + \sum_{i=1}^{B-1} e^{-d(h(r), h(\mathcal{F}_i))/\tau}}. \quad (6)$$

Here τ is a tuneable temperature parameter. To stabilize the training procedure and reach a non-trivial solution, the encoder applies different dropout masks to the reads and fragments similar to the method described in prior work [6]. Similar setups have been shown to work in written language applications, most notably in Sentence Transformers [40, 16, 35], which continue to be a strong benchmark for several downstream tasks requiring pre-trained sequence embeddings.

Encoder implementation

DNA-ESA uses a Transformer-encoder [12, 45], comprising 12 heads and 6-layers of encoder blocks. The size of the vocabulary is 10,000. Batch size B is set to 16 with gradient accumulation across 16 steps. Generated numerical representations for each read, $h(r) \in \mathbb{R}^{1020}$. The learning rate is annealed using one-cycle cosine annealing [42], dropout is set to 0.1, and $\tau = 0.05$. During training, the reference fragment $|\mathcal{F}_i| \sim \mathcal{U}([800, 2000])$ and read $|r_i| \sim \mathcal{U}([150, 500])$ have variable lengths sampled from a uniform distribution. Here, $|x|$ denotes the length of x . To improve model performance on noisy reads, 1 – 5% of bases are replaced with another random base in 40% of the reads in a batch. Shorter sequences were padded to equal the length of the longest sequence in a batch. The distance metric used is *Cosine Similarity*.

Search and retrieval

An outline of the search and retrieval process is presented in Fig. 4. Every read is encoded using the trained model and matched to reference fragments in the vector database. The top- K retrieved fragments per read are then aligned using a SW alignment library to find the optimal alignment. The following sections describe the indexing and retrieval part in more detail.

Indexing: For a given reference genome \mathcal{R} , we construct a minimal set of reference fragments $\mathcal{F} := \{\mathcal{F}_1, \mathcal{F}_2, \dots\}$ to span \mathcal{R} . Note that the fragments overlap at least a read length;

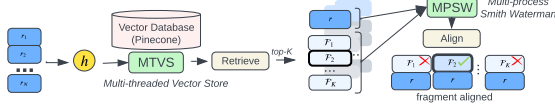


Fig. 4. System Overview [B] - Inference on a New Read: A read, as per (1) and generated by ART [19], is encoded by h . This is then compared to reference fragment representations in the vector database. The nearest- K fragments in the embedding space are retrieved for each read, and the optimal alignment is determined using (7).

i.e. $|\mathcal{F}_i \cap \mathcal{F}_{i+1}| \geq Q$ to guarantee that every read is fully contained within some fragment in the set. In our experiments with external read generators [19], $Q_{max} = 250$, $|\mathcal{F}_i| = 1250$. Each reference fragment is encoded using the trained *DNA-ESA* model, and the resulting sequence embeddings ($\in \mathbb{R}^{1020}$) – 3M vectors for a reference of 3B nucleotides – are inserted into a Pinecone database. Once populated with all the fragments, we are ready to perform the alignment.

Retrieval: Given a read r , we project its corresponding *DNA-ESA* representation into the vector store and retrieve the approximate nearest- K set of reference fragment vectors and the corresponding fragment metadata $\{\mathcal{F}_1, \mathcal{F}_2, \dots, \mathcal{F}_K\}$.

Diversity priors: While the top- K retrieved fragments can be drawn from across the entire vector store (genome), contemporary recommendation systems that use the top- K retrieval setup *rank and re-rank* top search results (*Slate Optimization* – see [49]) to ensure rich and diverse recommendations. Similarly, we apply a uniform prior wherein every retrieval step selects the top- K *per* chromosome.

Fine-Alignment: A standard SW distance library [9] is used to solve (4), which can be executed concurrently across the K -reference fragments. Let the optimal fragment be \mathcal{F}^* . The metadata for each vector includes (a) the raw \mathcal{F}^* sequence; (b) the start position of \mathcal{F}^* within the reference \mathcal{R} , $q_{\mathcal{F}^*|\mathcal{R}}$. Upon retrieval of a fragment and fine-alignment to find the fragment-level start index, $q_{|\mathcal{F}^*}$, the global reference start position is obtained as:

$$q^* = q_{|\mathcal{F}^*} + q_{\mathcal{F}^*|\mathcal{R}}. \quad (7)$$

Transformer-DNA baselines

This section outlines the setup for evaluating Transformer-DNA baselines, with their recall performance depicted in Fig. 1. We selected three architectures modeling nucleotide sequences: [NT] *NucleotideTransformer* ($\in \mathbb{R}^{1280}$) [11], [DB2] *DNABERT-2* ($\in \mathbb{R}^{768}$) [22], and [HD] *HyenaDNA* ($\in \mathbb{R}^{256}$) [36]. Each model employs mean- and max-pooling of token representations for sequence encoding ($2 \times 3 = 6$ baselines total). Independent vector stores for each baseline encode fragments from the entire 3gb genome. We sampled 40K pure reads of varying lengths ($Q \sim \mathcal{U}([25, 1000])$) and assessed the average recall for top-5, top-25, and top-50 fragments, as shown in Fig. 1. Overall, while baseline performance is modest, mean-pooling generally outperforms max-pooling, with DB2 (mean-pooled) and HD (max-pooled) as the most effective. These two baselines will be contrasted with *DNA-ESA* in Table 1.

DNA-ESA convergence plots are presented in Figs. 6a and 6b. Model checkpoints are available at OSF. In Fig. 2, representations of short 1,000-length sequences sampled from sequential (in-order) and gene-specific locations in the reference are visualized in a reduced 2D-UMAP [33]. The representation space demonstrates desired properties suitable for successfully

performing alignment: (a) Sequences sampled in order form a trajectory in the representation space: The loss function described in (6) encourages a pair of sequences *close* to one another to have a short distance between them in the representation space, and pairs further apart to have a larger distance. (b) Representations of sequences drawn from specific gene locations – despite not being close to one another – show gene-centric clustering: The *DNA-ESA* representation space partially acquires function-level separation as a byproduct of imposing *local* alignment constraints. The codebase is *linked*.

Sequence alignment of ART-simulated reads

The results from Sec. 3 demonstrate that even for pure reads, baseline models do not generate adequate representations to perform sequence alignment. In this section, *DNA-ESA* and the two best baselines – *DB2*, *mean* and *HD*, *max* – are evaluated using reads generated from an external read simulator (ART) – see [19]. ART has served as a reliable benchmark for evaluating other contemporary alignment tools and provides controls to model mutations and variations common in reads generated by Illumina machines.

Simulator configurations: The different simulation configuration options and settings are listed: (A) *Phred quality score* Q_{PH} in one of three $\{[10, 30], [30, 60], [60, 90]\}$ ranges: the likelihood of errors in base-calls of a generated read; (B) *Insertion rate* $I \in \{0, 10^{-2}\}$: the likelihood of adding a base to a random location in a read; (C) *Deletion rate* $D \in \{0, 10^{-2}\}$: the likelihood of deleting a base in the read; (Others): *Simulator system*: MSv3 [MiSeq]; *Read length*: 250.

Recall configurations: Once the top- K fragments have been retrieved, the first step is to solve (4), and for this, we need to compute the SW distance. For all presented results, the settings are: `match.score = -2`, `mismatch.penalty = +1`, `open.gap.penalty = +0.5`, `continue.gap.penalty = +0.1`. After alignment, we get q^* – see (7) – as the estimated location of a read in the genome. Let \hat{q}^* be its true location. If $q^* = \hat{q}^*$, it is a perfect match and the recall is successful. In cases where there is a mutation in the first or last position in a read, the fine-alignment will return $q_{\mathcal{F}^*}$ -offset by at most 2 locations, resulting in $\hat{q}^* = q^* \pm 2$. Hence, the condition for an exact location match: $|q^* - \hat{q}^*| \leq 2$.

Distance bound, $d_{SW} \in \{1\%, 2\%, 5\%\}$: It is well known that short fragments frequently repeat in the genome and q^* can correspond to the position of the read in a different location than from where it was sampled [29, 41]. In this case, $q^* \neq \hat{q}^*$, but the SW distance is the minimum possible. Moreover, when reads have mutations, the reference sequence corresponding to the read is no longer a perfect match. We define a bound d_{SW} for classifying whether a (read, retrieved fragment) pair is a successful alignment based on the SW distance between the pair (v^* – see Eq. 4) and the optimal SW distance as a particular read length Q :

$$d_{SW} = \frac{v^* - mQ}{(n - m)Q},$$

where $m(= -2)$ is the match score and $n(= +1)$ is the mismatch penalty, hyperparameters in the computation of the SW distance. We consider an alignment (with $Q = 250$) to be successful if the resulting SW distance between the read and the top returned fragment is within d_{SW} of the optimal for that read length. A $d_{SW} = 2\%$ (*default*) is equivalent to a mismatch of around 4 bases in a read of length 250.

Model	Settings	ART (MiSeqv3)				PacBio CCS ($\mu(v^*), \sigma(v^*)$)
		Search	[10,30]	[30,60]	[60,90]	Chr. 2, pbmm2 $d_{SW} = 5\%$
Transformer Architectures	HD (max)	K=50	13.20 ± 1.81	17.01 ± 2.01	18.03 ± 2.05	-
	DB2 (mean)		30.21 ± 2.44	39.19 ± 2.58	39.20 ± 2.58	-
	DNA-ESA (ours)	K=75	98.40 ± 0.71	98.64 ± 0.67	98.60 ± 0.67	97.5 ± 0.82
			98.80 ± 0.62	99.28 ± 0.52	98.88 ± 0.60	97.5 ± 0.82 (-498.0, 3.78)
Bowtie-2 (Classical)	-	99.80 ± 0.19			99.50 ± 0.43 (-497.9, 3.78)	
<i>diff.</i>	-	$<1\%$			$<2\%$	

Table 1. Performance of DNA-ESA with respect to baselines: The performance of DNA-ESA is compared to the DNA-BERT 2 and Hyena-DNA Transformer-based baseline models (with no additional finetuning) – the top performing baselines from Fig. 1. In addition, DNA-ESA is also compared with Bowtie-2 [25], a classical aligner. Comparisons are conducted across varying qualities (*Phred score*) of reads generated by ART [19]. Additionally, an external PacBio CCS dataset of ($Q = 250$ length-) reads from Chr. 2 of the Ashkenazim Trio - Son sample (as determined by pbmm2 [27]) are aligned using both Bowtie-2 and DNA-ESA. All baseline models utilize a dedicated vector store. For details on I, D, Q_{PH}, K, d_{SW} , refer to *Recall/Simulator Configurations*. Across models and ART-generated datasets, the performance of DNA-ESA supersedes other Transformer-based models and is comparable to Bowtie-2 to within 1%. With respect to reads from PacBio CCS, DNA-ESA performs with 2% of Bowtie-2 after controlling for the intrinsic quality of retrieved fragments according to the SW distance. Mean (μ) and standard deviation (σ) across the top SW distance values (v^*) of reads successfully aligned in the case of DNA-ESA and Bowtie-2 models are reported.

Performance

Table 1 reports the performance of DNA-ESA across several read generation configurations – we choose from one of three ranges of Phred score Q_{PH} , $\{[10, 30], [30, 60], [60, 90]\}$ – $I, D = 0.01, d_{SW} = 2\%$ – see Sec. 4), in addition to a direct comparison to DB2, mean and HD, max baselines (*without any further finetuning*), the best-performing baselines on pure reads identified in Sec. 3. In addition, we also compare DNA-ESA to Bowtie-2 [25], a conventional algorithmic aligner.

Additionally, models are also evaluated on an external set of reads from PacBio CCN generated on the Ashkenazim Trio (Son) (retrieved from the Genome in a Bottle resource (GIAB) [50]). For (ii), the raw reads are 10 kilobases long and for evaluation we consider random subset of 5000 reads associated to Chr. 2³ Reads input into the aligner are cropped randomly to a length of 250 to satisfy the computational requirements of DNA-ESA ($|\mathcal{F}_i \cap \mathcal{F}_{i+1}| = 250$).

We observe that: (A) DNA-ESA shows strong recall performance of $> 99\%$ across a variety of read generation and recall configurations; (B) On cleaner reads, DNA-ESA and Bowtie-2 are within $< 1\%$ of each other in recall while controlling for the quality of the retrieved alignments (as determined by the SW distance). The results indicate that this constitutes a new state-of-the-art model for Transformer-based sequence alignment.

Sweeping Top-K and the SW distance bound In Table 2, we report the performance of DNA-ESA across distance bounds $d_{SW} \in \{1\%, 2\%, 5\%\}$ and a number of recalled fragment settings $K \in \{25, 50, 75\}$. Distance bound $d_{SW} < 5\%$ is equivalent to an acceptable mismatch of at most ~ 8 bases between the read (length $Q = 250$) and recalled reference fragments. Recall rates are comparable with different d_{SW} values suggesting that when a read is successfully aligned, it is usually aligned to an objectively best match. Decreasing the

top- K per chromosome from $50 \rightarrow 25$ does not substantially worsen performance ($< 1\%$), indicating that the optimal retrievals are usually the closest in the embedding space. Additional ablation studies are presented in the Appendix.

Task transfer from Chromosome 2

Are these results indicative of DNA-ESA’s adaptability to new genomic sequences rather than strict adherence to its training data? This would suggest the model’s learning to solve the sequence alignment task rather than memorizing the genome.

Experiment setup: DNA-ESA is trained on Chromosome 2 – the longest chromosome – and recall is computed on unseen chromosomes from the human genome (3, Y) (*inter-chromosome*) and select chromosomes from chimpanzee (2A,2B) and rat (1,2) DNA (*inter-species*). Reads are generated with the following simulator configurations: $I = 10^{-2}, D = 10^{-2}, d_{SW} = 2\%, Q = 250$. Top- K is set to 50 / Chr., reads per setting = 5,000. Independent vector stores are constructed for each chromosome; representations for reference fragments (staging) and reads (testing) *are generated by the Chr. 2-trained model*. The results are reported in Tables 3, 4.

Performance: Details on convergence are in Appendix B. Table 3 shows that the performance on unseen human chromosomes (3, Y) is similar to the performance reported in Table 1, despite only training DNA-ESA on Chr. 2. This suggests DNA-ESA’s ability to generalize sequence alignment across chromosomes with different compositions. High Accuracy, Precision, and F1-scores further confirm the method’s specificity at this high recall. In Table 4, a trend of decreasing recall across species is observed: Human (2, 3, Y) $>$ Chimpanzee (2A, 2B) (Blue) $>$ Rat (1, 2), with chimpanzees likely performing better due to genetic similarities with humans [21]. Even distantly related species like *Thermus aquaticus* and *Acidobacteriota* show significant recall, highlighting DNA-ESA’s task transferability beyond simple data memorization.

³ Reads specific to a chromosome are filtered using the pbmm2 (Minimap) package [27].

I	D	$Q_{PH} \in [30, 60]$			$Q_{PH} \in [60, 90]$		
		$d_{SW} < 1\%$	$d_{SW} < 2\%$	$d_{SW} < 5\%$	$d_{SW} < 1\%$	$d_{SW} < 2\%$	$d_{SW} < 5\%$
Top-25 / chromosome							
0.0	0.0	97±0.94	98.12±0.76	98.56±0.69	97.24±0.91	97.96±0.80	98.6±0.69
	0.01	96.88±0.97	98±0.78	98.36±0.73	97.24±0.91	97.96±0.80	98.76±0.64
0.01	0.0	97.08±0.93	98.04±0.78	98.56±0.69	97±0.94	98.24±0.75	98.92±0.59
	0.01	97.16±0.80	97.96±0.56	99.2±0.52	97.6±0.85	98.12±0.76	98.76±0.62
Top-50 / chromosome							
0.0	0.0	97.52±0.86	99.04±0.57	99.08±0.57	98.2±0.75	98.88±0.59	99.16±0.52
	0.01	97.48±0.87	99.16±0.52	99.08±0.55	97.8±0.82	98.76±0.62	99.04±0.57
0.01	0.0	98.24±0.75	98.64±0.67	99.12±0.55	98.28±0.75	98.92±0.59	99.28±0.49
	0.01	97.72±0.83	98.64±0.67	99.36±0.46	97.84±0.92	98.6±0.66	99.0±0.57
Top-75 / chromosome							
0.0	0.0	98.04±0.78	99.12±0.55	99.0±0.57	98.4±0.71	99.12±0.55	98.4±0.71
	0.01	98.4±0.71	99.04±0.56	99.4±0.46	98.44±0.71	98.84±0.62	99.24±0.52
0.01	0.0	98.64±0.67	99.0±0.57	99.2±0.52	98.0±0.78	98.72±0.64	99.48±0.43
	0.01	98.68±0.64	99.28±0.49	99.4±0.46	98.48±0.69	98.88±0.59	99.4±0.46

Table 2. Sequence alignment recall of DNA-ESA sweeping top-K and d_{SW} : The various parameters are described in Sec. 4. DNA-ESA presents a recall of $> 99\%$ across several read configurations rivaling contemporary algorithmic models such as Bowtie. As expected, performance improves with larger search radius (top-K), higher quality reads (Q_{PH}) and large distance bound d_{SW} .

		Acc. \uparrow	F1 \uparrow	P \uparrow	R \uparrow		
Train	ART Reads	2 (seen in training)			3 (populated)	Y (populated)	
Chr. 2	$Q_{PH} \in [30, 60]$	99.74 \pm 0.29	99.74 \pm 0.29	99.99 \pm 0.01	99.49±0.46	98.87±0.59	99.99±0.01
Chr. 2	$Q_{PH} \in [60, 90]$	99.37 \pm 0.49	99.36 \pm 0.49	99.99 \pm 0.01	98.74±0.64	99.12±0.55	99.5±0.43

Table 3. DNA-ESA Performance on Chr. 2 and Task Transfer to Chr. 3, Y: DNA-ESA, trained on Chr. 2, is evaluated for aligning positive samples from Chr. 2 and negative samples from Chr. 3. Anticipated failure to align Chr. 3 reads (false positives) is due to significant SW distance. Metrics reported include weighted accuracy (Acc.), precision (P), F1-score (F1), and recall (R), for comparison with Table 1. [Grey] For Chr. 3 and Y, separate vector stores are populated using DNA-ESA representations learned using Chr. 2 {read,fragment} pairs. These results support the generalizing tendency of DNA-ESA to align sequences beyond the training reference.

Limitations and Future Work

DNA-ESA has the following challenges that we hope to overcome in future generations of the system: the computational speed, at 10K reads per minute, is a limiting factor for extensive genomic studies involving millions of reads. Despite this, the alignment task’s inherent parallelizability offers avenues for efficiency improvements. Our ongoing and future efforts are directed towards overcoming this time efficiency bottleneck, as detailed in Appendix Sec. C. We are considering various optimization strategies, including model compilation, to speed up inference and enhanced parallelization in vector store searches and fragment-read alignment. Additionally, we aim to enhance DNA-ESA’s performance at shorter read lengths, exploring alternative training methods and integrating more diverse read/reference features.

Concluding Remarks

Current DNA sequence alignment methods, honed over decades, incorporate DNA-specific enhancements in both indexing and retrieval, relying on algorithmic approaches. However, we introduce an alternative data-driven paradigm, employing a Transformer-based DNA-ESA encoder. Our method performs sequence alignment through self-supervised learning, utilizing contrastive loss. While similar methods

have previously found application in identifying approximate semantic similarity in written language, our approach surprisingly excels at identifying exact overlaps among DNA sequences. Empirical results underscore the model’s ability to embody the inherent structure of any DNA sequence, irrespective of location or species origin. A distinguishing feature of DNA-ESA is its ability to map both shorter reads and longer reference fragments into the same space by employing cosine similarity as a symmetric distance metric. This complements existing paradigms that have traditionally used a hierarchical and explicit comparison of base distributions.

DNA-ESA representations would find utility in other related tasks. If, for example, one had to align reads to the Pan Genome [31] instead of a single reference, one can populate a single vector store with fragments from all 47 genome assemblies. Then given a read, the nearest fragment to the read can belong to any reference variant. Note that in this case, we avoid having to construct a separate index for each of the references as is usually done in conventional methods.

One can similarly repurpose the representation space – originally intended for Sequence Alignment – to address the complementary task of Genome Assembly. We conclude this paper with a setup that provides initial proofpoints under reasonable simplifying assumptions about read lengths and overlaps among the reads. The resulting framework will be formalized and benchmarked with reads from actual experiments in our future work.

Species	$Q_{PH} \in [30, 60]$	$Q_{PH} \in [60, 90]$
	Recall Top-K @50 \uparrow	
<i>Thermus Aquaticus</i> [All]	99.9 \pm 0.01	99.9 \pm 0.01
<i>Acidobacteriota</i> [All]	99.9 \pm 0.01	99.9 \pm 0.01
<i>Rattus Norwegicus</i> [Chr. 1]	95.98 \pm 1.07	96.48 \pm 1.01
<i>Rattus Norwegicus</i> [Chr. 2]	97.99 \pm 0.78	96.49 \pm 1.01
<i>Pan Troglodytes</i> [Chr. 2A]	98.5 \pm 0.69	95.74 \pm 1.11
<i>Pan Troglodytes</i> [Chr. 2B]	95.99 \pm 1.08	96.25 \pm 1.05

Table 4. Cross-Species Task Transfer with DNA-ESA: Training on Human Chr. 2, Testing on Diverse Species: DNA-ESA, trained on human Chr. 2, aligns fragments and reads from different species, including *Rattus Norwegicus*, *Pan Troglodytes*, *Acidobacteriota*, and *Thermus Aquaticus*. These species, are evaluated for read alignment recall using ART-generated reads. The findings, consistent with Table 1, indicate DNA-ESA’s proficiency in modeling DNA sequence structure, beyond simply memorizing training data.

A setup for de-novo Genome Assembly using DNA-ESA

Consider a set of reads, $R := \{r_1, r_2, \dots, r_C\}$ from which we would like to estimate a reference \mathcal{R} . The de-novo assembly task is to estimate an ordering of the reads in R , $\hat{R} := (r_i, \dots, r_j, \dots, r_k)$ such that a concatenation (after removing overlaps) is approximately the original reference. In typical setups, all pairs of reads would need to be compared in order to find those that overlap and construct longer chains of the assembly in an incremental fashion. This may be visualized as a complete graph K_C with C nodes (reads) and C^2 edges (constraints). To avoid the quadratic complexity, modern techniques such as *Overlap-Layout-Consensus* (OLC) or *de Bruijn Graph* (DBG) approaches [30] have adopted hot-start heuristics such as base overlap and shared K-mer counts to reduce the number of pairwise read comparisons.

The representation space modeled by DNA-ESA admits a comparable assembly setup. Fig. 2 suggested emergent 1D manifolds in the representation space – comprising the embeddings of the reads – $h(r_1), h(r_2), \dots, h(r_C)$ – such that the relative *positions* of fragments along the manifold correlated to the relative *locations* of the fragments along the reference. *Therefore, a pairwise read-read comparison within a smaller radius in the embedding space would be sufficient to find reads that overlap.* And more generally, a walk along the 1D manifold would constitute a near-optimal assembly.

We provide an initial computational implementation of this idea: (a) The k-nearest neighbor (kNN) graph $G(R, d)$, representing the distances between close-by reads, is computed using the density-aware corrections provided by the UMAP library [33]: graph adjacency matrices for each of the chromosomes is visualized in Fig. 5. For this figure, the several reads are ordered manually as they appear in the assembly in order to highlight the connectivity pattern; the bright off-diagonal values indicate a chain-like structure corresponding to the observed manifold; (b) A *Hamiltonian* cycle computed through the graph that has the lowest total distance corresponds to an assembly, \hat{R} . This involves solving the Traveling Salesman Problem (TSP) – we use the 3/2-approximate Christofides algorithm [7]. After a walk across the reads is generated, a second pass through the walk greedily concatenates adjacent reads (r_i, r_{i+1}) by computing the alignment using the SW distance and removing duplicates and overlaps. In cases where adjacent reads do not have any alignment to one another – the walk isn’t guaranteed to be perfect since the DNA-ESA model is heuristical and the TSP algorithm is approximate – the current assembly part is stowed

away as a *contig* [17], and a new contig is instantiated with the incoming read. The fewer the contigs, the better the manifold in the representation space correlates to the ordering of the true reference.

Assembly is conducted across 4 of the shorter chromosomes in the *Thermus Aquaticus* genome. We consider (long) reads of length $Q = 500$, which have no indels, and the entire corpus of reads is ensured to have full coverage across each chromosome. Each read has an overlap of $\mathcal{U}([150, 250])$ bases with another read in the corpus of reads. QUASt [34] metrics are reported in Table 5.

N50 refers to the length of a contig (in bases) such that the contigs that exceed this length span 50% of the reference genome. NGA50 is a reference-aware N50 metric. The fewer contigs, large N(GA)50 scores in comparison to the large size of the chromosomes, when considered together, demonstrate that the reads are indeed ordered in a relative position-aware manner in the DNA-ESA embedding space with respect to a reference making the de-novo assembly task viable.

Appendix

A. Convergence

Fig. 6 plot the convergence of the DNA-ESA encoder model discussed in the main text. We see convergence after $\sim 20k$ steps.

B. Complexity of computing alignment

Cost of constructing a new representation

Computing the embedding \mathcal{E} of a sequence of length F using DNA-ESA encoding – a typical Transformer-based attention architecture – has the following computation complexity:

$$\mathcal{O}(LH * (F^2 * d + d^2 * F)) \Rightarrow \mathcal{O}(F^2 * d + d^2 * F) \quad (8)$$

Where d is the embedding dimension of the model, L is the number of layers in the Transformer and H is the number of heads per layer. As d is a controllable parameter for the model, we can further simplify:

$$\mathcal{O}(F^2 * d + d^2 * F) \Rightarrow \mathcal{O}(F^2) \quad (9)$$

The F^2 complexity follows the basic implementation of attention in transformers, but recent efforts [2, 24] have developed shortcuts to reduce the cost. These have already been applied to DNA sequence modeling [36].

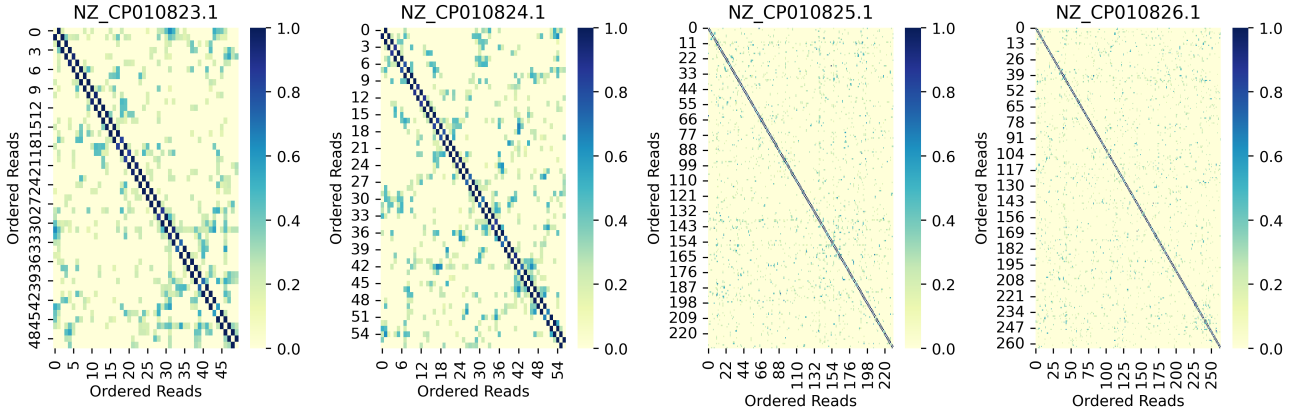
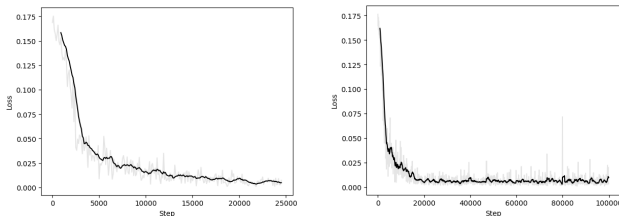


Fig. 5. Motivating the task of de-novo assembly using the distance adjacency matrix of the UMAP-generated k -nearest neighbor ($k = 10$) network of reads from *Thermus Aquaticus*: We assume that reads r_1, r_2, \dots, r_C belonging to a species are embedded into the DNA-ESA embedding space $h(r_1), h(r_2), \dots, h(r_C)$ using a model trained on a known reference genome belonging to a different species. For this illustrative numerical example we ensure that reads are created with the following properties: first, no read is a substring of any other read (efficient algorithms for the case where reads can be substrings of others will be covered in our future work); second every read has a corresponding read that it overlaps with for each end, and finally, the union of the reads cover the ground-truth reference genome. Thus, for every read r_i there exist reads r_k and r_j such that the ordered triplet (r_j, r_i, r_k) constitutes a fragment of the reference. In a perfect embedding scenario, the closest neighbors of r_i (i.e. $k = 1$ in an k -NN search) in the embedding space should be r_j and r_k . For this ideal case, if a network is constructed where each read (node) is connected to its two nearest neighbors, and the nodes are arranged based on the order in which they appear in the reference chromosome, one would get a bi-diagonal adjacency matrix. When ground truth is not known, the adjacency matrix will be a permuted version of a bi-diagonal matrix, but a complete assembly can still be performed by a greedy algorithm that starts with any node and pieces together the neighboring reads in the embedded space in time that grows linearly in the number of reads. Simulated reads, each of length 500 and with random overlaps of lengths drawn uniformly $\mathcal{U}([150, 250])$ with its neighboring reads at each end, are sampled from 4 of the chromosomes in *Thermus Aquaticus*, and are embedded into the DNA-ESA embedding space trained with a reference human genome. The sorted adjacency matrix of the UMAP [33]-generated k -NN ($k = 10$) network is presented above for each chromosome. The dark off-diagonal distance values in the k -NN adjacency graph with $k = 10$ show that the distance properties of actual embeddings of simulated reads from *Thermus Aquaticus* are almost coincident with that of the ideal case discussed above. Moreover, just as in the ideal case, by finding an approximate solution to the Traveling Salesman Problem in the unsorted network, one can find a walk (the assembly) that is close to the original reference. The results are presented in Table 5.

		Size (in kb) \uparrow	No. of Contigs \downarrow	N50 (in kb) \uparrow	NGA50 (in kb) \uparrow
Thermus Aquaticus	NZ_CP010823.1	14.4	1	14.4	14.4
	NZ_CP010824.1	16.6	1	16.6	16.6
	NZ_CP010825.1	69.9	22	6.0	4.4
	NZ_CP010826.1	78.7	15	10.3	10.3

Table 5. DNA-ESA performance on de-novo assembly of the *Thermus Aquaticus* genome: The solution to the approximate TSP applied on the DNA-ESA read-read network generates a set of contigs that can be evaluated with respect to the original reference using QUAST [34]. For the two shorter chromosomes, the resulting assembly was perfect; the entire reference is encapsulated by one contig. Even in the case with longer chromosomes, the number of contigs are still few and of significant length (as indicated by the high N(G)50 score) suggesting a strong correlation between the distance metric in the embedding space and the ordering of the corresponding reads in the assembly.



(a) Trained on the Human Genome (b) Trained on the Human Chromosome 2

Fig. 6. DNA-ESA convergence plots. Both plots show the loss pr. step (grey). For clarity, we smooth the loss using a moving average (black).

Vector Store Upstream

Vector store \mathcal{D} is populated once (in bulk) with encoded fragment-length sequences drawn from the entire genome; constant time complexity C to upload $< 10M$ vectors.

Retrieval Cost

Given a new embedding, $\epsilon(G, K)$ is the cost of retrieving top- K nearest neighbors across the fragment embeddings, where G is the length of the reference genome. In modern vector databases, where several hashing techniques such as approximate K -nearest neighbors are used, ϵ scales logarithmically with G . This is indeed the key benefit of using such databases.

I	D	$Q_{PH} \in [30, 60]$			$Q_{PH} \in [60, 90]$		
		$d_{SW} < 1\%$	$d_{SW} < 2\%$	$d_{SW} < 5\%$	$d_{SW} < 1\%$	$d_{SW} < 2\%$	$d_{SW} < 5\%$
Top-1250 $\sim 50 \times \{\text{Chr. 22, X, Y, M}\}$							
0.0	0.0	98.56 \pm 0.67	97.60 \pm 0.85	98.56 \pm 0.67	97.76 \pm 0.82	97.76 \pm 0.82	97.44 \pm 0.88
0.01	0.01	98.8 \pm 0.62	98.4 \pm 0.71	98.8 \pm 0.62	99.2 \pm 0.52	98.4 \pm 0.71	98.4 \pm 0.71
Top-50 <i>global</i>							
0.0	0.0	91.6 \pm 1.49	92.4 \pm 1.43	93.8 \pm 1.31	90.4 \pm 1.58	93.8 \pm 1.31	94.8 \pm 1.21
0.01	0.01	89.6 \pm 1.64	91.6 \pm 1.49	96 \pm 1.07	94.4 \pm 1.25	94.4 \pm 1.25	93.2 \pm 1.36

Table 6. Sequence alignment recall of DNA-ESA - without diversity priors: The various parameters are described in Sec. 4. When compared to the main results presented in Table 1, it is evident that the addition of diversity priors results in an improvement of \sim in recall. Similar to the result presented in the main text, performance improves with larger search radius in the vector store (top- K), higher quality reads (Q_{PH}) and large distance bound (d_{SW}).

Fine-grained Alignment

Existing libraries/algorithms (e.g. the Smith–Waterman algorithm) can identify the alignment between a fragment sequence (of length F) and read (of length Q) in $\mathcal{O}(FQ)$.

Total Complexity

Total complexity involves (a) constructing the representation of a read; (b) querying the vector store; (c) running fine-grained alignment with respect to the K returned reference fragment sequences:

$$\begin{aligned} \mathcal{O}(F^2 + FQK + \epsilon(G, K)) &\Rightarrow \mathcal{O}(F(F + QK) + \epsilon(G, K)) \\ &\Rightarrow \mathcal{O}(FQK + \epsilon(G, K)) \end{aligned}$$

C. Ablation studies

Without diversity priors in top-K

In Table 6, we report the performance without diversity priors used in the retrieval step: i.e. the nearest- K neighbors in the embedding space are selected from the *entire* set of fragments spanning the genome rather than uniformly sampling from each chromosome. The performance predictably falls in comparison to those reported in Table 1 since fewer fragments scattered unevenly across the different chromosomes are being retrieved per read.

Across read lengths

In Table 7, the performance of DNA-ESA is reported across read lengths. We observe *Zero-shot performance at longer read lengths*: The model performs better at longer read lengths (even exceeding the read length bound established during training $\mathcal{U}[150, 500]$); while evaluating for longer reads, we make sure to guarantee that the reads exist as subsequences of fragments. Improving the performance at shorter read lengths is the subject of future work.

Competing interests

No competing interest is declared.

Author contributions statement

VR devised the task and framework and assisted with writing. MP aided in writing and bridging NLP and Bioinformatics

communities. LSB contributed to writing and brainstorming. PH and KCE realized the framework and assisted with writing. SR ran several experiments to improve model performance. LM and TG reviewed existing conventional baselines.

References

- Alexei Baevski, Henry Zhou, Abdelrahman Mohamed, and Michael Auli. wav2vec 2.0: A framework for self-supervised learning of speech representations, 2020.
- Iz Beltagy, Matthew E. Peters, and Arman Cohan. Longformer: The long-document transformer. *arXiv preprint arXiv:2004.05150*, 2020.
- Rishi Bommasani, Drew A. Hudson, Ehsan Adeli, Russ Altman, Simran Arora, Sydney von Arx, Michael S. Bernstein, Jeannette Bohg, Antoine Bosselut, Emma Brunskill, Erik Brynjolfsson, Shyamal Buch, Dallas Card, Rodrigo Castellon, Niladri Chatterji, Annie Chen, Kathleen Creel, Jared Quincy Davis, Dora Demszky, Chris Donahue, Moussa Doumbouya, Esin Durmus, Stefano Ermon, John Etchemendy, Kawin Ethayarajh, Li Fei-Fei, Chelsea Finn, Trevor Gale, Lauren Gillespie, Karan Goel, Noah Goodman, Shelby Grossman, Neel Guha, Tatsunori Hashimoto, Peter Henderson, John Hewitt, Daniel E. Ho, Jenny Hong, Kyle Hsu, Jing Huang, Thomas Icard, Saahil Jain, Dan Jurafsky, Pratyusha Kalluri, Siddharth Karamcheti, Geoff Keeling, Fereshte Khani, Omar Khattab, Pang Wei Koh, Mark Krass, Ranjay Krishna, Rohith Kudithipudi, Ananya Kumar, Faisal Ladhak, Mina Lee, Tony Lee, Jure Leskovec, Isabelle Levent, Xiang Lisa Li, Xuechen Li, Tengyu Ma, Ali Malik, Christopher D. Manning, Suvir Mirchandani, Eric Mitchell, Zanele Munyikwa, Suraj Nair, Avaniika Narayan, Deepak Narayanan, Ben Newman, Allen Nie, Juan Carlos Niebles, Hamed Nilforoshan, Julian Nyarko, Giray Ogut, Laurel Orr, Isabel Papadimitriou, Joon Sung Park, Chris Piech, Eva Portelance, Christopher Potts, Aditi Raghunathan, Rob Reich, Hongyu Ren, Frieda Rong, Yusuf Roohani, Camilo Ruiz, Jack Ryan, Christopher Ré, Dorsa Sadigh, Shiori Sagawa, Keshav Santhanam, Andy Shih, Krishnan Srinivasan, Alex Tamkin, Rohan Taori, Armin W. Thomas, Florian Tramèr, Rose E. Wang, William Wang, Bohan Wu, Jiajun Wu, Yuhuai Wu, Sang Michael Xie, Michihiro Yasunaga, Jiaxuan You, Matei Zaharia, Michael Zhang, Tianyi Zhang, Xikun Zhang, Yuhui Zhang, Lucia Zheng, Kaitlyn Zhou, and Percy Liang. On the opportunities and risks of foundation models, 2022.

I	D	Q = 200	Q = 225	Q = 250
$Q_{PH} \in [30, 60]$				
0	0	99 ± 0.57	98.6 ± 0.67	99 ± 0.57
0.01	0.01	97.4 ± 0.88	98.8 ± 0.62	98.6 ± 0.67
$Q_{PH} \in [60, 90]$				
0	0	98.6 ± 0.67	98.6 ± 0.67	98.9 ± 0.59
0.01	0.01	98.6 ± 0.67	99 ± 0.57	98.6 ± 0.67

Table 7. DNA-ESA recall performance across read lengths: Performance of DNA-ESA is higher for longer reads including those lengths on which the model was not trained ($Q \in \mathcal{U}([150, 500])$). Shorter reads are more challenging for the model potentially due to replicates found across the reference.

4. Tom B. Brown, Benjamin Mann, Nick Ryder, Melanie Subbiah, Jared Kaplan, Prafulla Dhariwal, Arvind Neelakantan, Pranav Shyam, Girish Sastry, Amanda Askell, Sandhini Agarwal, Ariel Herbert-Voss, Gretchen Krueger, Tom Henighan, Rewon Child, Aditya Ramesh, Daniel M. Ziegler, Jeffrey Wu, Clemens Winter, Christopher Hesse, Mark Chen, Eric Sigler, Mateusz Litwin, Scott Gray, Benjamin Chess, Jack Clark, Christopher Berner, Sam McCandlish, Alec Radford, Ilya Sutskever, and Dario Amodei. Language models are few-shot learners, 2020.
5. Ting Chen, Simon Kornblith, Mohammad Norouzi, and Geoffrey Hinton. A simple framework for contrastive learning of visual representations. In *International conference on machine learning*, pages 1597–1607. PMLR, 2020.
6. Ting Chen, Simon Kornblith, Mohammad Norouzi, and Geoffrey Hinton. A simple framework for contrastive learning of visual representations. In *International conference on machine learning*, pages 1597–1607. PMLR, 2020.
7. Nicos Christofides. Worst-case analysis of a new heuristic for the travelling salesman problem. *Operations Research Forum*, 3, 1976.
8. C. J. Clopper and E. S. Pearson. The Use of Confidence or Fiducial Limits illustrated in the case of the binomial. *Biometrika*, 26(4):404–413, 12 1934.
9. Peter J. A. Cock, Tiago Antao, Jeffrey T. Chang, Brad A. Chapman, Cymon J. Cox, Andrew Dalke, Iddo Friedberg, Thomas Hamelryck, Frank Kauff, Bartek Wilczynski, and Michiel J. L. de Hoon. Biopython: freely available Python tools for computational molecular biology and bioinformatics. *Bioinformatics*, 25(11):1422–1423, 03 2009.
10. Zhuyun Dai, Vincent Y Zhao, Ji Ma, Yi Luan, Jianmo Ni, Jing Lu, Anton Bakalov, Kelvin Guu, Keith B Hall, and Ming-Wei Chang. Promptagator: Few-shot dense retrieval from 8 examples. *arXiv preprint arXiv:2209.11755*, 2022.
11. Hugo Dalla-Torre, Liam Gonzalez, Javier Mendoza Revilla, Nicolas Lopez Carranza, Adam Henryk Grywaczewski, Francesco Oteri, Christian Dallago, Evan Trop, Hassan Sirelkhatim, Guillaume Richard, et al. The nucleotide transformer: Building and evaluating robust foundation models for human genomics. *bioRxiv*, pages 2023–01, 2023.
12. Jacob Devlin, Ming-Wei Chang, Kenton Lee, and Kristina Toutanova. BERT: Pre-training of Deep Bidirectional Transformers for Language Understanding. In *Proceedings of the 2019 Conference of the North American Chapter of the Association for Computational Linguistics: Human Language Technologies, Volume 1 (Long and Short Papers)*, pages 4171–4186, Minneapolis, Minnesota, June 2019. Association for Computational Linguistics.
13. Alexey Dosovitskiy, Lucas Beyer, Alexander Kolesnikov, Dirk Weissenborn, Xiaohua Zhai, Thomas Unterthiner, Mostafa Dehghani, Matthias Minderer, Georg Heigold, and Sylvain Gelly. An image is worth 16x16 words: Transformers for image recognition at scale. *arXiv preprint arXiv:2010.11929*, 2020.
14. Alexey Dosovitskiy, Lucas Beyer, Alexander Kolesnikov, Dirk Weissenborn, Xiaohua Zhai, Thomas Unterthiner, Mostafa Dehghani, Matthias Minderer, Georg Heigold, Sylvain Gelly, Jakob Uszkoreit, and Neil Houlsby. An image is worth 16x16 words: Transformers for image recognition at scale, 2021.
15. Veniamin Fishman, Yuri Kuratov, Maxim Petrov, Aleksei Shmelev, Denis Shepelin, Nikolay Chekanov, Olga Kardymon, and Mikhail Burtsev. GENA-LM: A Family of Open-Source Foundational Models for Long DNA Sequences. *bioRxiv*, pages 2023–06, 2023. Publisher: Cold Spring Harbor Laboratory.
16. Tianyu Gao, Xingcheng Yao, and Danqi Chen. SimCSE: Simple Contrastive Learning of Sentence Embeddings. In *Proceedings of the 2021 Conference on Empirical Methods in Natural Language Processing*, pages 6894–6910, Online and Punta Cana, Dominican Republic, November 2021. Association for Computational Linguistics.
17. Simon G Gregory. *Contig Assembly*. John Wiley & Sons, Ltd, 2005.
18. Raia Hadsell, Sumit Chopra, and Yann LeCun. Dimensionality reduction by learning an invariant mapping. In *2006 IEEE computer society conference on computer vision and pattern recognition (CVPR’06)*, volume 2, pages 1735–1742. IEEE, 2006.
19. Weichun Huang, Leping Li, Jason R. Myers, and Gabor T. Marth. ART: a next-generation sequencing read simulator. *Bioinformatics*, 28(4):593–594, 2012. Publisher: Oxford University Press.
20. David A. Huffman. A method for the construction of minimum-redundancy codes. *Proceedings of the IRE*, 40(9):1098–1101, 1952. Publisher: IEEE.
21. JW Ijdo, Antonio Baldini, DC Ward, ST Reeders, and RA Wells. Origin of human chromosome 2: an ancestral telomere-telomere fusion. *Proceedings of the National Academy of Sciences*, 88(20):9051–9055, 1991.
22. Yanrong Ji, Zhihan Zhou, Han Liu, and Ramana V. Davuluri. DNABERT: pre-trained Bidirectional Encoder Representations from Transformers model for DNA-language in genome. *Bioinformatics*, 37(15):2112–2120, 2021. Publisher: Oxford University Press.

23. Jeff Johnson, Matthijs Douze, and Hervé Jégou. Billion-scale similarity search with gpus. *IEEE Transactions on Big Data*, 7(3):535–547, 2019. Publisher: IEEE.
24. Nikita Kitaev, Lukasz Kaiser, and Anselm Levskaya. Reformer: The efficient transformer. *arXiv preprint arXiv:2001.04451*, 2020.
25. Ben Langmead, Christopher Wilks, Valentin Antonescu, and Rone Charles. Scaling read aligners to hundreds of threads on general-purpose processors. *Bioinformatics*, 35(3):421–432, 07 2018.
26. Patrick Lewis, Ethan Perez, Aleksandra Piktus, Fabio Petroni, Vladimir Karpukhin, Naman Goyal, Heinrich Küttler, Mike Lewis, Wen-tau Yih, Tim Rocktäschel, et al. Retrieval-augmented generation for knowledge-intensive nlp tasks. *Advances in Neural Information Processing Systems*, 33:9459–9474, 2020.
27. Heng Li. Minimap2: pairwise alignment for nucleotide sequences. *Bioinformatics*, 34(18):3094–3100, 05 2018.
28. Heng Li and Richard Durbin. Fast and accurate short read alignment with burrows–wheeler transform. *bioinformatics*, 25(14):1754–1760, 2009.
29. Wentian Li and Jan Freudenberg. Mappability and read length. *Frontiers in Genetics*, 5, 2014.
30. Zhenyu Li, Yanxiang Chen, Desheng Mu, Jianying Yuan, Yujian Shi, Hao Zhang, Jun Gan, Nan Li, Xuesong Hu, Binghang Liu, Bicheng Yang, and Wei Fan. Comparison of the two major classes of assembly algorithms: overlap–layout–consensus and de-bruijn-graph. *Briefings in Functional Genomics*, 11(1):25–37, 12 2011.
31. Wen-Wei Liao, Mobin Asri, Jana Ebler, Daniel Doerr, Marina Haukness, Glenn Hickey, Shuangjia Lu, Julian K Lucas, Jean Monlong, Haley J Abel, et al. A draft human pangenome reference. *Nature*, 617(7960):312–324, 2023.
32. Udi Manber and Gene Myers. Suffix arrays: a new method for on-line string searches. *siam Journal on Computing*, 22(5):935–948, 1993. Publisher: SIAM.
33. Leland McInnes, John Healy, and James Melville. Umap: Uniform manifold approximation and projection for dimension reduction. *arXiv preprint arXiv:1802.03426*, 2018.
34. Alla Mikheenko, Andrey Prjibelski, Vladislav Saveliev, Dmitry Antipov, and Alexey Gurevich. Versatile genome assembly evaluation with QUAST-LG. *Bioinformatics*, 34(13):i142–i150, 06 2018.
35. Niklas Muennighoff, Nouamane Tazi, Loic Magne, and Nils Reimers. MTEB: Massive Text Embedding Benchmark. In *Proceedings of the 17th Conference of the European Chapter of the Association for Computational Linguistics*, pages 2014–2037, Dubrovnik, Croatia, May 2023. Association for Computational Linguistics.
36. Eric Nguyen, Michael Poli, Marjan Faizi, Armin Thomas, Callum Birch-Sykes, Michael Wornow, Aman Patel, Clayton Rabideau, Stefano Massaroli, and Yoshua Bengio. Hyenadna: Long-range genomic sequence modeling at single nucleotide resolution. *arXiv preprint arXiv:2306.15794*, 2023.
37. Sergey Nurk, Sergey Koren, Arang Rhie, Mikko Rautiainen, Andrey V. Bzikadze, Alla Mikheenko, Mitchell R. Vollger, Nicolas Altemose, Lev Uralsky, Ariel Gershman, Sergey Aganezov, Savannah J. Hoyt, Mark Diekhans, Glennis A. Logsdon, Michael Alonge, Stylianos E. Antonarakis, Matthew Borchers, Gerard G. Bouffard, Shelise Y. Brooks, Gina V. Caldas, Nae-Chyun Chen, Haoyu Cheng, Chen-Shan Chin, William Chow, Leonardo G. de Lima, Philip C. Dishuck, Richard Durbin, Tatiana Dvorkina, Ian T. Fiddes, Giulio Formenti, Robert S. Fulton, Arkarachai Fungtammasan, Erik Garrison, Patrick G. S. Grady, Tina A. Graves-Lindsay, Ira M. Hall, Nancy F. Hansen, Gabrielle A. Hartley, Marina Haukness, Kerstin Howe, Michael W. Hunkapiller, Chirag Jain, Miten Jain, Erich D. Jarvis, Peter Kerpedjiev, Melanie Kirsche, Mikhail Kolmogorov, Jonas Korlach, Milinn Kremitzki, Heng Li, Valerie V. Maduro, Tobias Marshall, Ann M. McCartney, Jennifer McDaniel, Danny E. Miller, James C. Mullikin, Eugene W. Myers, Nathan D. Olson, Benedict Paten, Paul Peluso, Pavel A. Pevzner, David Porubsky, Tamara Potapova, Evgeny I. Rogaez, Jeffrey A. Rosenfeld, Steven L. Salzberg, Valerie A. Schneider, Fritz J. Sedlazeck, Kishwar Shafin, Colin J. Shew, Alaina Shumate, Ying Sims, Arian F. A. Smit, Daniela C. Soto, Ivan Sović, Jessica M. Storer, Aaron Streets, Beth A. Sullivan, Françoise Thibaud-Nissen, James Torrance, Justin Wagner, Brian P. Walenz, Aaron Wenger, Jonathan M. D. Wood, Chunlin Xiao, Stephanie M. Yan, Alice C. Young, Samantha Zarate, Urvashi Surti, Rajiv C. McCoy, Megan Y. Dennis, Ivan A. Alexandrov, Jennifer L. Gerton, Rachel J. O’Neill, Winston Timp, Justin M. Zook, Michael C. Schatz, Evan E. Eichler, Karen H. Miga, and Adam M. Phillippy. The complete sequence of a human genome. *Science*, 376(6588):44–53, 2022.
38. Baolin Peng, Michel Galley, Pengcheng He, Hao Cheng, Yujia Xie, Yu Hu, Qiuyuan Huang, Lars Liden, Zhou Yu, Weizhu Chen, and Jianfeng Gao. Check your facts and try again: Improving large language models with external knowledge and automated feedback, 2023.
39. Xipeng Qiu, Tianxiang Sun, Yige Xu, Yunfan Shao, Ning Dai, and Xuanjing Huang. Pre-trained models for natural language processing: A survey. *Science China Technological Sciences*, 63(10):1872–1897, 2020.
40. Nils Reimers and Iryna Gurevych. Sentence-BERT: Sentence Embeddings using Siamese BERT-Networks. In *Proceedings of the 2019 Conference on Empirical Methods in Natural Language Processing and the 9th International Joint Conference on Natural Language Processing (EMNLP-IJCNLP)*, pages 3982–3992, Hong Kong, China, November 2019. Association for Computational Linguistics.
41. Mikhail V Simkin and Vwani P Roychowdhury. Re-inventing willis. *Physics Reports*, 502(1):1–35, 2011.
42. Leslie N. Smith and Nicholay Topin. Super-convergence: Very fast training of neural networks using large learning rates. In *Artificial intelligence and machine learning for multi-domain operations applications*, volume 11006, pages 369–386. SPIE, 2019.
43. Ian Tenney, Dipanjan Das, and Ellie Pavlick. Bert rediscovers the classical nlp pipeline, 2019.
44. Md. Vasimuddin, Sanchit Misra, Heng Li, and Srinivas Aluru. Efficient architecture-aware acceleration of bwa-mem for multicore systems. In *2019 IEEE International Parallel and Distributed Processing Symposium (IPDPS)*, pages 314–324, 2019.
45. Ashish Vaswani, Noam Shazeer, Niki Parmar, Jakob Uszkoreit, Llion Jones, Aidan N. Gomez, Lukasz Kaiser, and Illia Polosukhin. Attention is all you need. *Advances in neural information processing systems*, 30, 2017.
46. Prateek Verma and Jonathan Berger. Audio transformers: Transformer architectures for large scale audio understanding. adieu convolutions. *arXiv preprint arXiv:2105.00335*, 2021.

-
47. Christopher Wang, Vighnesh Subramaniam, Adam Uri Yaari, Gabriel Kreiman, Boris Katz, Ignacio Cases, and Andrei Barbu. BrainBERT: Self-supervised representation learning for intracranial recordings. *arXiv preprint arXiv:2302.14367*, 2023.
 48. Zhihan Zhou, Yanrong Ji, Weijian Li, Pratik Dutta, Ramana Davuluri, and Han Liu. Dnabert-2: Efficient foundation model and benchmark for multi-species genome, 2023.
 49. Xiaojin Zhu, Andrew B Goldberg, Jurgen Van Gael, and David Andrzejewski. Improving diversity in ranking using absorbing random walks. In *Human Language Technologies 2007: The Conference of the North American Chapter of the Association for Computational Linguistics; Proceedings of the Main Conference*, pages 97–104, 2007.
 50. Justin M Zook, David Catoe, Jennifer McDaniel, Lindsay Vang, Noah Spies, Arend Sidow, Ziming Weng, Yuling Liu, Christopher E Mason, Noah Alexander, et al. Extensive sequencing of seven human genomes to characterize benchmark reference materials. *Scientific data*, 3(1):1–26, 2016.
 51. Maxim Zvyagin, Alexander Brace, Kyle Hippe, Yuntian Deng, Bin Zhang, Cindy Orozco Bohorquez, Austin Clyde, Bharat Kale, Danilo Perez-Rivera, and Heng Ma. GenSLMs: Genome-scale language models reveal SARS-CoV-2 evolutionary dynamics. *bioRxiv*, pages 2022–10, 2022. Publisher: Cold Spring Harbor Laboratory.